

# Journal of Visualized Experiments

## Evaluating the electrochemical properties of supercapacitors using the three-electrode system

--Manuscript Draft--

|  |   |
|--|---|
| Article Type:  | Invited Methods Collection - JoVE Produced Video  |
| Manuscript Number:   | JoVE63319R2   |
| Full Title:  | Evaluating the electrochemical properties of supercapacitors using the three-electrode system                   |
| Corresponding Author:  | Inho Nam, Ph.D.<br>Chung-Ang University - Seoul Campus: Chung-Ang University<br>Seoul, Seoul KOREA, REPUBLIC OF |
| Corresponding Author's Institution:  | Chung-Ang University - Seoul Campus: Chung-Ang University   |
| Corresponding Author E-Mail:   | inhonam@cau.ac.kr   |
| Order of Authors:  | Inho Nam, Ph.D.<br>Hojong Eom<br>Jihyeon Kang<br>Seohyeon Jang<br>Ohhyun Kwon<br>Seyoung Choi<br>Junhyeop Shin  |
| Additional Information:  |   |
| Question   | Response  |
| Please specify the section of the submitted manuscript.  | Engineering   |
| Please indicate whether this article will be Standard Access or Open Access.   | Standard Access (\$1400)  |
| Please indicate the <b>city, state/province, and country</b> where this article will be <b>filmed</b> . Please do not use abbreviations. | Seoul, Republic of Korea  |
| Please confirm that you have read and agree to the terms and conditions of the author license agreement that applies below:              | I agree to the <a href="#">Author License Agreement</a>   |
| Please confirm that you have read and agree to the terms and conditions of the video release that applies below:                         | I agree to the <a href="#">Video Release</a>  |
| Please provide any comments to the journal here.   |   |

**TITLE:**

Evaluating the Electrochemical Properties of Supercapacitors using the Three-Electrode System

**AUTHORS AND AFFILIATIONS:**

Hojong Eom, Jihyeon Kang, Seohyeon Jang, Ohhyun Kwon, Seyoung Choi, Junhyeop Shin, Inho Nam

School of Chemical Engineering and Materials Science, Department of Intelligent Energy and Industry, Chung-Ang University, Seoul 06974, Republic of Korea

Email addresses of co-authors:

|               |                         |
|---------------|-------------------------|
| Hojong Eom    | (ehj5738@cau.ac.kr)     |
| Jihyeon Kang  | (kar04114@cau.ac.kr)    |
| Seohyeon Jang | (tjgus6142@cau.ac.kr)   |
| Ohhyun Kwon   | (ohram2@cau.ac.kr)      |
| Seyoung Choi  | (chy5376@cau.ac.kr)     |
| Junhyeop Shin | (wnsguqdl123@cau.ac.kr) |
| Inho Nam      | (inhonam@cau.ac.kr)     |

Corresponding author:

Inho Nam (inhonam@cau.ac.kr)

**SUMMARY:**

The protocol describes the evaluation of various electrochemical properties of supercapacitors using a three-electrode system with a potentiostat device.

**ABSTRACT:**

The three-electrode system is a basic and general analytical platform for investigating the electrochemical performance and characteristics of energy storage systems at the material level. Supercapacitors are one of the most important emergent energy storage systems developed in the past decade. Here, the electrochemical performance of a supercapacitor was evaluated using a three-electrode system with a potentiostat device. The three-electrode system consisted of a working electrode (WE), reference electrode (RE), and counter electrode (CE). The WE is the electrode where the potential is controlled and the current is measured, and it is the target of research. The RE acts as a reference for measuring and controlling the potential of the system, and the CE is used to complete the closed circuit to enable electrochemical measurements. This system provides accurate analytical results for evaluating electrochemical parameters such as the specific capacitance, stability, and impedance through cyclic voltammetry (CV), galvanostatic charge-discharge (GCD), and electrochemical impedance spectroscopy (EIS). Several experimental design protocols are proposed by controlling the parameter values of the sequence when using a three-electrode system with a potentiostat device to evaluate the electrochemical performance of supercapacitors. Through these protocols, the researcher can set up a three-electrode system to obtain reasonable electrochemical results for assessing the performance of supercapacitors.

## INTRODUCTION:

Supercapacitors have attracted enormous attention as suitable power sources for a variety of applications such as microelectronic devices, electric vehicles (EVs), and stationary energy storage systems. In EV applications, supercapacitors can be used for rapid acceleration and can enable the storage of regenerative energy during the deceleration and braking processes. In renewable energy fields, such as solar power generation<sup>1</sup> and wind power generation<sup>2</sup>, supercapacitors can be used as stationary energy storage systems<sup>3,4</sup>. Renewable energy generation is limited by the fluctuating and intermittent nature of these energy supplies; therefore, an energy storage system that can respond immediately during irregular power generation is required<sup>5</sup>. Supercapacitors, which store energy *via* mechanisms that differ from those of lithium-ion batteries, exhibit a high power density, stable cycle performance, and fast charging–discharging<sup>6</sup>. Depending on the storage mechanism, supercapacitors can be distinguished into double-layer capacitors (EDLCs) and pseudocapacitors<sup>7</sup>. EDLCs accumulate electrostatic charge at the electrode surface. Therefore, the capacitance is determined by the amount of charge, which is affected by the surface area and porous structure of the electrode materials. By contrast, pseudocapacitors, which consist of conducting polymers and metal oxide materials, store charge through a Faradaic reaction process. The various electrochemical properties of supercapacitors are related to the electrode materials, and developing new electrode materials is the main issue in improving the performance of supercapacitors<sup>8</sup>. Hence, evaluating the electrochemical properties of these new materials or systems is important in the progress of research and further applications in real life. In this regard, electrochemical evaluation using a three-electrode system is the most basic and widely utilized method in lab-scale research of energy storage systems<sup>9–13</sup>.

The three-electrode system is a simple and reliable approach for evaluating the electrochemical properties, such as the specific capacitance, resistance, conductivity, and cycle life of supercapacitors<sup>14</sup>. The system offers the benefit of enabling analysis of the electrochemical characteristics of single materials<sup>15</sup>, which is in contrast to the two-electrode system, where the characteristics can be studied through the analysis of the given material. The two-electrode system just gives information about the reaction between two electrodes. It is suitable for analyzing the electrochemical properties of the entire energy storage system. The potential of the electrode is not fixed. Therefore, it is not known at what voltage the reaction takes place. However, three-electrode system analyzes only one electrode with fixing potential which can perform a detailed analysis of the single electrode. Therefore, the system is targeted toward analyzing the specific performance at the material level. The three-electrode system consists of a working electrode (WE), reference electrode (RE), and counter electrode (CE)<sup>16,17</sup>. The WE is the target of research, assessment as it performs the electrochemical reaction of interest<sup>18</sup> and is composed of a redox material that is of potential interest. In the case of EDLCs, utilizing high surface area materials is the main issue. Therefore, porous materials with a high surface area and micropores, such as porous carbon, graphene, and nanotubes, are preferred<sup>19,20</sup>. Activated carbon is the most common material for EDLCs because of its high specific area ( $>1000\text{ m}^2/\text{g}$ ) and many micropores. Pseudocapacitors are fabricated with materials that can undergo a Faradaic reaction<sup>21</sup>. Metal oxides ( $\text{RuO}_x$ ,  $\text{MnO}_x$ , etc.) and conducting polymers (PANI, PPy, etc.) are commonly used<sup>22</sup>. The RE and CE are used to analyze the electrochemical properties of the WE.

The RE serves as a reference for measuring and controlling the potential of the system; the normal hydrogen electrode (NHE) and Ag/AgCl (saturated KCl) are generally chosen as the RE<sup>23</sup>. The CE is paired with the WE and completes the electrical circuit to allow charge transfer. For the CE, electrochemically inert materials are used, such as platinum (Pt) and gold (Au)<sup>24</sup>. All components of the three-electrode system are connected to a potentiostat device, which controls the potential of the entire circuit.

Cyclic voltammetry (CV), galvanostatic charge-discharge (GCD), and electrochemical impedance spectroscopy (EIS) are typical analytical methods that use a three-electrode system. Various electrochemical characteristics of supercapacitors can be assessed using these methods. CV is the basic electrochemical method used to investigate the electrochemical behavior (electron transfer coefficient, reversible or irreversible, etc.) and capacitive properties of material during repeated redox processes<sup>14,24</sup>. The CV plot shows redox peaks related to the reduction and oxidation of the material. Through this information, researchers can evaluate the electrode performance and determine the potential where the material is reduced and oxidized. Furthermore, through CV analysis, it is possible to determine the amount of charge that material or electrode can store. The total charge is a function of the potential, and the capacitance can be easily calculated<sup>6,18</sup>. Capacitance is the main issue in supercapacitors. A higher capacitance represents the ability to store more charge. EDLCs give rise to rectangular CV patterns with linear lines so that the capacitance of the electrode can be calculated easily. Pseudocapacitors present redox peaks in rectangular plots. Based on this information, researchers can assess the electrochemical properties of materials using CV measurements<sup>18</sup>.

GCD is a commonly employed method for identifying the cycle stability of an electrode. For long-term use, the cycle stability should be verified at a constant current density. Each cycle consists of charge-discharge steps<sup>14</sup>. Researchers can determine the cycle stability through variations in the charge-discharge graph, specific capacitance retention, and Coulombic efficiency. EDLCs give rise to a linear pattern; thus, the specific capacitance of the electrode can be calculated easily using the slope of the discharge curve<sup>6</sup>. However, pseudocapacitors exhibit a nonlinear pattern. The discharge slope varies during the discharging process<sup>7</sup>. Furthermore, the internal resistance can be analyzed through the current-resistance (IR) drop, which is the potential drop owing to the resistance<sup>6,25</sup>.

EIS is a useful method for identifying the impedance of energy storage systems without destruction of the sample<sup>26</sup>. The impedance can be calculated by applying a sinusoidal voltage and determining the phase angle<sup>14</sup>. The impedance is also a function of the frequency. Therefore, the EIS spectrum is acquired over a range of frequencies. At high frequencies, kinetic factors such as the internal resistance and charge transfer are operative<sup>24,27</sup>. At low frequencies, the diffusion factor and Warburg impedance can be detected, which are related to mass transfer and thermodynamics<sup>24,27</sup>. EIS is a powerful tool for analyzing the kinetic and thermodynamic properties of a material at the same time<sup>28</sup>. This study describes the analysis protocols for evaluating the electrochemical performance of supercapacitors using a three-electrode system.

## 133 PROTOCOL:

### 135 1. Fabrication of electrode and supercapacitor (Figure 1)

137 1.1. Prepare the electrodes prior to the electrochemical analysis by combining 80 weight (wt)%  
138 of the electrode active material (0.8 g activated carbon), 10 wt% of the conductive material (0.1  
139 g carbon black), and 10 wt% of the binder (0.1 g polytetrafluoroethylene (PTFE)).

141 1.1.1. Drop isopropanol (IPA; 0.1–0.2 mL) into the above-mentioned mixture, then spread the  
142 mixture thinly into a dough with a roller.

144 1.2. Before attaching the electrode to stainless steel (SUS) mesh, cut the SUS mesh to  
145 dimensions of 1.5 cm (width) × 5 cm (length). After weighing the SUS mesh, coat the electrode (1  
146 cm<sup>2</sup>) with a thickness of 0.1–0.2 mm on a SUS mesh and compress it with an electrode pressing  
147 machine. Here, the mass range of the electrode was 0.001–0.003 g.

149 1.3. Dry the assembled supercapacitor electrode in an oven at 80 °C for about 1 day to  
150 evaporate the IPA.

152 1.4. Weigh the SUS mesh to obtain the weight of the electrode and then immerse the mesh  
153 in the electrolyte (2 M H<sub>2</sub>SO<sub>4</sub> aqueous solution).

155 1.5. Place the SUS mesh in a desiccator to remove air bubbles at the surface of the  
156 supercapacitor electrode.

### 158 2. Preparation of sequence file for electrochemical analysis

160 2.1. CV sequence settings to obtain the analysis results.

162 2.1.1. Run the potentiostat measurement program to set the measurement experiment  
163 sequence file (Figure 2A).

165 2.1.2. Click the **Experiment** button in the toolbar and go to **Sequence File Editor > New** or click  
166 the **New Sequence** button (Figure 2B). Click the **Add** button to add a sequence step (Figure 3A).

168 2.1.3. In every step, set **Control** as **Sweep**, **Configuration** as **PSTAT**, **Mode** as **CYCLIC**, and **Range**  
169 as **Auto**. Set the **Reference** for **Initial(V)** and **Middle(V)** as **Eref** and put **-200e-3** in the **Value**. Set  
170 the **Reference** for **Final(V)** as **Eref** and put **800e-3** in the **Value**.

172 2.1.4. The voltage scan rate is set as the desired value by the user. Here, the scan rates were set  
173 to 10, 20, 30, 50, and 100 mV/s. Put the value in **Scanrate(V/s)** as **10.0000e-3**, **20.000e-3**,  
174 **30.000e-3**, **50.000e-3**, and **100.00e-3** respectively.

176 2.1.5. Set **Quiet time(s)** as **0** and **Segments** as the number **2n+1** where n is the number of cycles.

Here, 21 was applied for 10 cycles.

2.1.6. Set **Cut Off Condition** as follows: for **Condition-1** set **Item** as **Step End** and **Go Next** as **Next**.

2.1.7. In the **Controlling Miscellaneous Setting** section, in the **Sampling** tab, set **Item** as **Times(s)**, **OP** as **>=**, and **DeltaValue** as **0.333333**, **0.166666**, **0.111111**, **0.06667**, and **0.03333** for each scan rate. This is the time interval for recording the data.

2.1.8. Click **Save As** to save the CV analysis sequence file in any folder of the computer.

## 2.2. GCD sequence settings to obtain the analysis results

2.2.1. Run the potentiostat measurement program to set the measurement experiment sequence file (**Figure 2A**).

2.2.2. Click the **Experiment** button in the toolbar and go to **Sequence File Editor > New** or click the **New Sequence** button (**Figure 2B**). Click the **Add** button to add a sequence step (**Figure 4A,B**).

2.2.3. In **Step-1**, set **Control** as **CONSTANT**, Configuration as **GSTAT**, **Mode** as **NORMAL**, and **Range** as **Auto**. Set the **Reference for Current(A)** as **ZERO**. When the mass of the electrode is 0.00235 g, set **Value** as **1.8618e-3** which means the current density is 1 A/g.

2.2.4. Set **Cut Off Condition** as follow: for **Condition-1** set **Item** as **Voltage**, **OP** as **>=**, **DeltaValue** as **800e-3**, and **Go Next** as **Next**.

2.2.5. Set the following in the **Controlling Miscellaneous setting** section: in the **Sampling** tab, set **Item** as **Times(s)**, **OP** as **>=**, and **DeltaValue** as **0.1**.

2.2.6. In **Step-2**, each set is the same as in **Step-1**, except set value of **Current(A)** as the negative value of **Step-1** ( **-1.8618e-3**). Set **Condition-1** as follows: **Item** as **Voltage**, **OP** as **<=**, **DeltaValue** as **-200e-3**, and **Go Next** as **Next**.

2.2.7. In **Step-3**, set **Control** as **LOOP**, Configuration as **CYCLE**, and set **List-1** in **Condition-1** of **Cut Off Condition** as **Loop Next**, **Go Next** as **Step-1**, and set **List-2** as **Step End**, and **Go Next** as **Next**. Set the **Iteration** value as **10** which is the number of repeating cycles.

2.2.8. **Step-1, step-2, and step-3** form a single loop. Copy and paste them after **step-4** and change the value of **Current (A)** to either **3.7236e-3**, **5.5855e-3**, **9.3091e-3**, or **18.618e-3**, calculated for various current densities of 2,3,5, and 10 A/g.

2.2.9. Click **Save As** to save the GCD analysis sequence file in any folder of the computer.

## 2.3. EIS sequence settings to obtain the analysis results

2.3.1. Run the potentiostat measurement program to set the measurement experiment sequence file (**Figure 2A**).

2.3.2. Click the **Experiment** button in the toolbar and go to **Sequence File Editor > New** or click the **New Sequence** button (**Figure 2B**). Click the **Add** button to add a sequence step (**Figure 5A,B**).

2.3.3. In **Step-1**, set **Control** as **CONSTANT**, **Configuration** as **PSTAT**, **Mode** as **TIMER STOP**, and **Range** as **Auto**. Set the **Reference for Voltage(V)** as **Eref** and **Value** as **500e-3** which is half of the size of the voltage range.

2.3.5. Set cut-off condition as follows: for **Condition-1** set **Item** as **Step Time**, **OP** as **>=**, **DeltaValue** as **3:00**, and **Go Next** as **Next**. This is the process for stabilizing the potentiostat device.

2.3.6. In **Step-2**, set **Control** as **EIS**, **Configuration** as **PSTAT**, **Mode** as **LOG**, and **Range** as **Auto**. Set **Speed of Initial (Hz)** as **Normal** and value of **Initial (Hz)** and **Middle (Hz)** as **1.0000e+6** which is the high-frequency value and **Final (Hz)** as **10.000e-6**, which is the low-frequency value.

2.3.7. Set the **Reference for Bias(V)** as **Eref** and **Value** as **500e-3**. To get a linear response result, set the **amplitude (Vrms)** as **10.000e-3**. Set **Density** as **10** and **Iteration** as **1**.

2.3.8. Click **Save as** to save the EIS analysis sequence file in any folder of the computer.

### 3. Electrochemical analysis

3.1. Operate the potentiostat device and run the measurement program to perform the CV, GCD, and EIS analyses. Fill 100 mL of 2 M H<sub>2</sub>SO<sub>4</sub> aqueous electrolyte in a glass container (a beaker-shaped glass container was used).

3.2. Before starting the measurement, in the potentiostat, connect the three types of lines: the working electrode (L-WE), the reference electrode (L-RE), and the counter electrode (L-CE), to the SUS mesh, reference electrode (Ag/AgCl), and counter electrode (Pt wire), respectively (**Figure 6**). Connect the fourth line, the working sensor (L-WS) to the L-WE.

3.3. Cover the glass container with a cap, and immerse the three electrodes in the electrolyte through a perforation in the cap. Position the electrodes so that the WE is maintained at a constant distance between the CE and RE.

3.4. Run the measurement program and open the prepared sequence. Click **Apply to CH** to insert the sequence to the potentiostat's channel. Start the measurement by clicking the **Start** button.

### 4. Data analysis

#### 4.1. CV data analysis for fitting the graph

4.1.1. Open raw measurement data in the convert program to obtain the results in spreadsheet format. Click the **File** button and open the raw data. Select all cycles and click **Export ASCII** on the toolbar. Check the **Cycle**, **Voltage**, and **Current** in **Columns to Export** on the right side of the program.

4.1.2. Click **Create Directory** and then click **Export** to convert raw data to spreadsheet format.

4.1.3. Open the spreadsheet file and extract the voltage and current values of cycles 10, 20, 30, 40, and 50, which are the last cycles at each scan rate.

4.1.4. Plot the CV graph with the voltage as the X-axis and specific current density as the Y-axis.

#### 4.2. GCD data analysis for fitting the graph

4.2.1. Open raw measurement data in the convert program to obtain the results in spreadsheet format. Click the **File** button and open the raw data. Select all cycles and click **Export ASCII** on the toolbar. Check the **Cycle**, **Voltage**, and **CycleTime** in **Columns to Export** on the right side of the program.

4.2.2. Click **Create Directory** and then click **Export** to convert raw data to spreadsheet format.

4.2.3. Open the spreadsheet file and extract the voltage and CycleTime values for cycles 10, 20, 30, 40, and 50, which are the last cycles at each current density.

4.2.4. Plot the GCD graph with the cycle time as the X-axis and voltage as the Y-axis.

#### 4.3. EIS data analysis for fitting the graph

4.3.1. Open raw measurement data in EIS program. Click the **Open file** icon and open raw data and click the file name that was applied to see the detailed data.

4.3.2. Extract Frequency [Hz] as the X value and Z' [Ohm] as the Y value and plot the EIS graph.

### REPRESENTATIVE RESULTS:

The electrodes were manufactured according to protocol step 1 (**Figure 1**). Thin and homogeneous electrodes were attached to SUS mesh with a size of 1 cm<sup>2</sup> and 0.1–0.2 mm thickness. After drying, the weight of the pure electrode was obtained. The electrode was immersed in a 2 M H<sub>2</sub>SO<sub>4</sub> aqueous electrolyte, and the electrolyte was allowed to sufficiently permeate the electrode before the electrochemical analyses. The production sequence and system setting for the electrochemical measurements were performed according to protocol steps 2 and 3 (**Figure 2 – Figure 5**). The glass container used in the system can have various shapes<sup>29</sup> where the distance between each electrode is minimized. The measurement results



were organized and interpreted according to protocol step 4. To confirm whether the analysis was successful, the real-time graph obtained during the analysis and the shape of the graph of the raw data obtained after the analysis should be checked (**Figures 3B,4C,5C**). In the case of CV, a box-shaped graph was obtained at 300 mV/s, whereas GCD showed a symmetrical triangle. In the case of EIS, it is possible to check whether the analysis is properly performed through the size of the equivalent series resistance and semicircle, and the pattern at a low frequency depending on the material characteristics.

**Figure 7** presents the CV, GCD, and EIS data. CV is the most common technique for determining the capacitance of electrodes and the characteristics of materials as a function of the potential. The well-developed rectangle-shaped CV graph in the scan rate range from 10 to 200 mV/s indicates EDLC characteristics and confirms that the supercapacitor operated well as an EDLC with good rate capability<sup>30</sup> (**Figure 7A**). However, when the scan rate was above 300 mV/s, the graph lost its rectangular shape and collapsed, which means that the electrode lost the EDLC characteristics (**Figure 7B**). The specific capacitance of supercapacitors can be calculated from the CV data at each scan rate using the following equation<sup>6</sup>:

$$C_{sp} = \frac{1}{v(V_2 - V_1)} \int_{V_1}^{V_2} I(V) dV \quad (1)$$

where  $C_{sp}$ ,  $v$ ,  $V_1$ ,  $V_2$ , and  $I(V)$  are the specific capacitance, scan rate, discharge voltage limit, charge voltage limit, and voltammogram current density (A/g), respectively. The specific capacitance was 126, 109, 104, 97, and 87 F/g at respective scan rates of 10, 20, 30, 50, and 100 mV/s.

GCD can be used to determine the cycle stability and resistance parameters of the electrode. As shown in **Figure 7C**, the GCD graph of the electrode presented a symmetric linear profile<sup>31</sup> in all current densities within the potential range from -0.2 to 0.8 V. This is also a characteristic property of EDLCs. Subsequently, as the current density increased, the time on the x-axis decreased, and the area of the triangle decreased. The specific capacitance was calculated by dividing the discharge time by the voltage and multiplying by the current density, giving values of 153, 140, 135, 120, and 110 F/g at the respective current densities of 1, 2, 3, 5, and 10 A/g. The internal resistance ( $R_{ESR}$ ) was calculated using the following equation<sup>32</sup>:

$$R_{ESR} = \frac{\Delta V}{2 \cdot I} \quad (2)$$

where  $\Delta V$  is the IR drop, which is the potential drop due to the resistance (this is an additive effect of the cell components and electrolytes<sup>6,25</sup>), and  $I$  is the current density. The value of  $R_{ESR}$  was 0.00565  $\Omega$  at a current density of 1 A/g. The long-cycle test can be used to determine the cycle stability of the WE. The cycle stability is one of the main issues in energy storage systems when applied to an electrical device and can be confirmed by repeating many cycles at a constant current density. As shown in **Figure 7D**, the AC WE showed 99.2% capacitance retention over 10000 cycles at a current density of 10 A/g.

The EIS graphs are plotted in **Figure 7E,F**. EIS is a useful method for identifying the resistance of

cell systems without destruction. The impedance of the cell is a function of the frequency (the typical frequency range is from 100 kHz to 10 MHz) with a small voltage (5 mV or 10 mV)<sup>14,33</sup>. In addition, the Nyquist plot is a common way to represent the impedance data, where the imaginary/real part of the impedance is plotted in the frequency range. The resulting data are recorded from the high-frequency domain to the low-frequency domain, and each part represents various types of resistance<sup>6</sup>. As shown in **Figure 7E**, the Nyquist plot can be divided into four parts. Part A corresponds to the equivalent series resistance, which is known as the sum of the resistance of the bulk electrolyte<sup>34,35</sup> and the contact resistance between the electrode and the current collector<sup>36,37</sup>. Part B presents a semicircle, the diameter of which reflects the electrolyte resistance in the pores of the electrodes<sup>38</sup> or charge transfer resistance<sup>34</sup>. Furthermore, the sum of parts A and B can be interpreted as the internal resistance, which is the sum of the bulk electrolyte resistance and the charge transfer resistance<sup>36</sup>. In part C, the 45° line region indicates the ion transport limitation of the electrode structures in the electrolyte<sup>34,39</sup> or ion transport limitation in the bulk electrolyte<sup>35</sup>. Lastly, the vertical line in part D (**Figure 7F**) is attributed to the dominant capacitive behavior of the electric double layer formed at the electrode/electrolyte interface<sup>40</sup>. The EIS graph for the example system showed very small equivalent series resistance and semicircle ( $R_{ct}$ ) values, and the shape at low frequencies appeared close to vertical, which indicates the EDLC characteristics of the device<sup>6,41</sup>.

#### FIGURES AND TABLE LEGENDS:

**Figure 1. Fabricating process of supercapacitor.** (A) Prepare the materials for electrode and mix with IPA. (B) Make an electrode in the form of a dough. (C) Spread the electrode thinly, cut it into 1 cm<sup>2</sup> size with a thickness of 0.1–0.2 mm, and attach it to the stainless steel (SUS) mesh. (D) Immerse the supercapacitor in electrolyte after pressing and drying. Abbreviations: PTFE= polytetrafluoroethylene; IPA= isopropanol.

**Figure 2. Run the program for sequence settings.** (A) Run the analysis program and (B) create the new sequence file with the editor.

**Figure 3. CV sequence settings.** (A) CV sequence setting for each scan rate and (B) real-time measurement CV graphs.

**Figure 4. GCD sequence settings.** (A, B) GCD sequence setting for each current density and (C) real-time measurement GCD graphs.

**Figure 5. EIS sequence settings.** (A, B) EIS sequence setting and (C) real-time measurement EIS graph.

**Figure 6. The basic composition of the three-electrode system for electrochemical measurement.**

**Figure 7. Electrochemical analyses graphs.** (A) CV at low scan rates (10 mV/s – 100 mV/s); (B) CV at high scan rates (200 mV/s – 1000 mV/s); (C) GCD at a current density from 1 to 10 A/g; (D) Long cycle test at the current density of 10 A/g; (E, F) EIS Nyquist plots.

## DISCUSSION:

This study provides a protocol for various analyses using a three-electrode system with a potentiostat device. This system is widely used to evaluate the electrochemical performance of supercapacitors. A suitable sequence for each analysis (CV, GCD, and EIS) is important for obtaining optimized electrochemical data. Compared with the two-electrode system having a simple setup, the three-electrode system is specialized for analyzing supercapacitors at the material level<sup>15</sup>. However, the selection of appropriate experimental parameters such as the electrolyte<sup>42</sup>, potential range<sup>43</sup>, scan rate<sup>14</sup>, and current density<sup>14</sup> is important for obtaining high-quality data. The parameters that must be judiciously set are summarized below.

The weight ratio may vary depending on the type of material used. The ratio can be adjusted according to the properties of the conductive material and binder used. The best ratio must maximize the amount of active material while maintaining the electrical conductivity and mechanical strength of the electrode. An 80 wt% ratio of the active material is widely used<sup>44-47</sup>. The potential range is dependent on the electrochemical stability window (ESW) of the electrolyte. The ESW of an electrolyte can be determined by its reduction and oxidation potentials, which define the stable range within which the electrolyte can be used without decomposition<sup>48,49</sup>. The potential window for aqueous electrolytes is usually below 1.23 V, which is restricted by the thermodynamic potential of water electrolysis<sup>50</sup>. In the case of organic electrolytes, the potential window depends on the organic solvent used; organic electrolytes have a high voltage window (2.6 to 4.0 V)<sup>51</sup>. Researchers should set the optimal potential range in sequence according to the chosen electrolyte. In the case of an electrolyte that reacts upon contact with air, the container must be sealed.

The scan rate is the potential that varies linearly with the scan speed<sup>18</sup> and has a crucial effect on the voltammetric behavior of materials. The optimal scan rate range cannot be specified because it depends on the material. At a higher scan rate, more redox reactions occur, and if the redox reaction is too fast, it is difficult to measure the electrochemical properties of the materials. At a lower scan rate, some peaks may be missing because there is sufficient time for activation during the redox reaction<sup>14</sup>. Researchers can select and adjust the optimal range using reference and empirical data. A scan rate from 50 mV/s to 1 V/s is commonly used. The current density is another parameter that affects the electrochemical parameters, including the capacitance<sup>14</sup>. If the current density is too high, the operating voltage is hardly measured. It is one of the reasons that the capacitance and energy density is decreased. An appropriate current density can be determined from the CV graph. The range of the y-axis shown for each scan rate may be used as the current density. A repeated cycle is applied in CV and GCD analyses to obtain the steady-state data. The cycle required to reach the steady state differs depending on the properties of the material. During cycling, the system attempts to achieve the equilibrium state and struggles to reach the same pattern<sup>14</sup>. Selecting a sufficient number of cycles for the materials is important. Ten cycles were applied in the present experiment.

Each parameter must be carefully determined because each parameter influences the next parameter value. Selecting the parameter values for obtaining optimal electrochemical data may involve modifying variables based on the initial experimental results. Evaluation of the

electrochemical performance of a supercapacitor using the three-electrode system provides reliable data based on the values that the researcher has entered, but it is solely up to the user to set suitable parameters for analysis. The protocols specified in this report and the explanations supporting them will aid researchers in making a more informed decision.

To evaluate the electrochemical performance of supercapacitors, the mixing ratio of the electrode material and the electrode weight are vital parameters in the final step. The specific capacitance and current density can be obtained from the exact loading amount of the active material using the weight information. Inaccurate weight information may cause errors in the results. Finally, the installation of the appropriate equipment is important. The respective electrodes should not come into contact, but the distance between each electrode is indicated by the resistance of the system. Therefore, the electrodes should be placed as close as possible<sup>29</sup>. It is necessary to minimize external factors that may affect the evaluation of the supercapacitor by determining whether the electrode connection parts are corroded, or if the RE and the CE are in good condition.

The three-electrode system can perform detailed analysis, but through this, all performance of the supercapacitor cannot be evaluated. As mentioned earlier, the three-electrode system analyzes only one electrode at the material level. The final supercapacitor system consists of symmetrical or asymmetric electrodes and requires further evaluation of this system for application to real-life and industry. Many studies have conducted an evaluation using a three-electrode and two-electrode system together<sup>52-55</sup>. The system is also changing depending on the application. Not just evaluating supercapacitor, it is widely used in fuel cells<sup>56,57</sup> and surface treatment<sup>58,59</sup> fields. Various changes are taking place, such as giving flexibility<sup>60</sup> or deviating from the existing form to another form<sup>61</sup>. The materials' characteristics can be easily evaluated with this system. Therefore, it will be applied in various forms to fields that require material analysis and evaluation.

In this paper, a supercapacitor was fabricated according to the proposed protocol. In addition, we evaluated the performance of a supercapacitor at the material level using various electrochemical analyses by utilizing the three-electrode system. The electrochemical properties of the electrodes were determined by adjusting the sequence parameters. This basic electrochemical protocol using the three-electrode system can be used to guide manufacturing and evaluation techniques for supercapacitor testing for beginners in this field of research.

#### **ACKNOWLEDGMENTS:**

This work was supported by the Korea Institute of Energy Technology Evaluation and Planning (KETEP) and the Ministry of Trade, Industry & Energy (MOTIE) of the Republic of Korea (No. 20214000000280), and the Chung-Ang University Graduate Research Scholarship 2021.

#### **DISCLOSURES:**

The authors have nothing to disclose.

#### **REFERENCES:**

484 1 El-Kady, M. F. et al. Engineering three-dimensional hybrid supercapacitors and  
485 microsupercapacitors for high-performance integrated energy storage. *Proceedings of the*  
486 *National Academy of Sciences*. **112** (14), 4233 (2015).

487 2 Gee, A. M., Robinson, F. V. P., Dunn, R. W. Analysis of Battery Lifetime Extension in a  
488 Small-Scale Wind-Energy System Using Supercapacitors. *IEEE Transactions on Energy Conversion*.  
489 **28** (1), 24–33 (2013).

490 3 Zhang, Z. et al. A high-efficiency energy regenerative shock absorber using  
491 supercapacitors for renewable energy applications in range extended electric vehicle. *Applied*  
492 *Energy*. **178**, 177–188 (2016).

493 4 Libich, J., Máca, J., Vondrák, J., Čech, O., Sedlářiková, M. Supercapacitors: Properties and  
494 Applications. *Journal of Energy Storage*. **17**, 224–227 (2018).

495 5 Cheng, Y. Super capacitor applications for renewable energy generation and control in  
496 smart grids. *2011 IEEE International Symposium on Industrial Electronics*. 1131–1136 (2011).

497 6 Mathis, T. S. et al. Energy Storage Data Reporting in Perspective—Guidelines for  
498 Interpreting the Performance of Electrochemical Energy Storage Systems. *Advanced Energy*  
499 *Materials*. **9** (39), 1902007 (2019).

500 7 González, A., Goikolea, E., Barrena, J. A., Mysyk, R. Review on supercapacitors:  
501 Technologies and materials. *Renewable and Sustainable Energy Reviews*. **58**, 1189–1206, (2016).

502 8 Yang, L. et al. Emergence of melanin-inspired supercapacitors. *Nano Today*. **37**, 101075  
503 (2021).

504 9 Hendel, S. J., Young, E. R. Introduction to Electrochemistry and the Use of  
505 Electrochemistry to Synthesize and Evaluate Catalysts for Water Oxidation and Reduction.  
506 *Journal of Chemical Education*. **93** (11), 1951–1956 (2016).

507 10 Licht, F., Aleman Milán, G., Andreas, H. A. Bringing Real-World Energy-Storage Research  
508 into a Second-Year Physical-Chemistry Lab Using a MnO<sub>2</sub>-Based Supercapacitor. *Journal of*  
509 *Chemical Education*. **95** (11), 2028–2033 (2018).

510 11 Jakubowska, A. A Student-Constructed Galvanic Cell for the Measurement of Cell  
511 Potentials at Different Temperatures. *Journal of Chemical Education*. **93** (5), 915–919 (2016).

512 12 González-Flores, D., Montero, M. L. An Advanced Experiment for Studying Electron  
513 Transfer and Charge Storage on Surfaces Modified with Metallic Complexes. *Journal of Chemical*  
514 *Education*. **90** (8), 1077–1081 (2013).

515 13 Da Silva, L. M. et al. Reviewing the fundamentals of supercapacitors and the difficulties  
516 involving the analysis of the electrochemical findings obtained for porous electrode materials.  
517 *Energy Storage Materials*. **27**, 555–590 (2020).

518 14 Choudhary, Y. S., Jothi, L., Nageswaran, G. Electrochemical Characterization.  
519 *Spectroscopic Methods for Nanomaterials Characterization*. Elsevier. 19–54 (2017).

520 15 Girard, H.-L., Dunn, B., Pilon, L. Simulations and Interpretation of Three-Electrode Cyclic  
521 Voltammograms of Pseudocapacitive Electrodes. *Electrochimica Acta*. **211**, 420–429 (2016).

522 16 Bard, A. J., Inzelt, G., Scholz, F. *Electrochemical Dictionary*. Springer. (2012).

523 17 Bard, A. J., Faulkner, L. R. *Electrochemical methods: fundamentals and applications*. Wiley.  
524 (2000).

525 18 Elgrishi, N. et al. A Practical Beginner's Guide to Cyclic Voltammetry. *Journal of Chemical*  
526 *Education*. **95** (2), 197–206 (2018).

527 19 Shiraishi, S., Tanaike, O. Application of Carbon Materials Derived from Fluorocarbons in

528 an Electrochemical Capacitor. *Advanced Fluoride-Based Materials for Energy Conversion*.  
529 Elsevier. 415–430 (2015).

530 20 Inagaki, M., Kang, F. in *Materials Science and Engineering of Carbon: Fundamentals*.  
531 Butterworth-Heinemann Publishing. (2014).

532 21 Fleischmann, S. et al. Pseudocapacitance: From Fundamental Understanding to High  
533 Power Energy Storage Materials. *Chemical Reviews*. **120** (14), 6738–6782 (2020).

534 22 Miao, Y.-E. & Liu, T. in *Electrospinning: Nanofabrication and Applications*. William Andrew  
535 Publishing. 641–669 (2019).

536 23 Yin, J., Qi, L., Wang, H. Antifreezing Ag/AgCl reference electrodes: Fabrication and  
537 applications. *Journal of Electroanalytical Chemistry*. **666**, 25–31 (2012).

538 24 Bard, A.J., Faulkner, L.R. *Electrochemical Methods: Fundamentals and Applications*. Wiley.  
539 New York (2001).

540 25 Wang, W. et al. Electrochemical cells for medium- and large-scale energy storage:  
541 fundamentals. *Advances in Batteries for Medium and Large-Scale Energy Storage*. Woodhead  
542 Publishing. 3–28 (2015).

543 26 Mansfeld, F. Use of electrochemical impedance spectroscopy for the study of corrosion  
544 protection by polymer coatings. *Journal of Applied Electrochemistry*. **25** (3), 187–202 (1995).

545 27 Murbach, M. D., Hu, V. W., Schwartz, D. T. Nonlinear Electrochemical Impedance  
546 Spectroscopy of Lithium-Ion Batteries: Experimental Approach, Analysis, and Initial Findings.  
547 *Journal of The Electrochemical Society*. **165** (11), A2758–A2765 (2018).

548 28 Macdonald, J. R., Johnson, W. B. in *Impedance Spectroscopy*. 1–26 (2005).

549 29 Chen, S. in *Handbook of Electrochemistry*. Elsevier. 3–56 (2007).

550 30 Xi, S., Zhu, Y., Yang, Y., Jiang, S., Tang, Z. Facile Synthesis of Free-Standing NiO/MnO<sub>2</sub> Core-  
551 Shell Nanoflakes on Carbon Cloth for Flexible Supercapacitors. *Nanoscale Research Letters*. **12**  
552 (1), 171 (2017).

553 31 Kim, M., Oh, I., Kim, J. Superior electric double layer capacitors using micro- and  
554 mesoporous silicon carbide sphere. *Journal of Materials Chemistry A*. **3** (7), 3944–3951 (2015).

555 32 Stoller, M. D., Ruoff, R. S. Best practice methods for determining an electrode material's  
556 performance for ultracapacitors. *Energy & Environmental Science*. **3** (9), 1294–1301 (2010).

557 33 Taberna, P. L., Simon, P., Fauvarque, J. F. Electrochemical Characteristics and Impedance  
558 Spectroscopy Studies of Carbon-Carbon Supercapacitors. *Journal of The Electrochemical Society*.  
559 **150** (3), A292 (2003).

560 34 Yang, I., Kim, S.-G., Kwon, S. H., Kim, M.-S., Jung, J. C. Relationships between pore size and  
561 charge transfer resistance of carbon aerogels for organic electric double-layer capacitor  
562 electrodes. *Electrochimica Acta*. **223**, 21–30 (2017).

563 35 Arulepp, M. et al. Influence of the solvent properties on the characteristics of a double  
564 layer capacitor. *Journal of Power Sources*. **133** (2), 320–328 (2004).

565 36 Mei, B.-A., Munteshari, O., Lau, J., Dunn, B., Pilon, L. Physical Interpretations of Nyquist  
566 Plots for EDLC Electrodes and Devices. *The Journal of Physical Chemistry C*. **122** (1), 194–206  
567 (2018).

568 37 Nian, Y.-R., Teng, H. Influence of surface oxides on the impedance behavior of carbon-  
569 based electrochemical capacitors. *Journal of Electroanalytical Chemistry*. **540**, 119–127 (2003).

570 38 Gamby, J., Taberna, P. L., Simon, P., Fauvarque, J. F., Chesneau, M. Studies and  
571 characterisations of various activated carbons used for carbon/carbon supercapacitors. *Journal*

572 of Power Sources. **101** (1), 109–116 (2001).

573 39 Coromina, H. M., Adeniran, B., Mokaya, R., Walsh, D. A. Bridging the performance gap  
574 between electric double-layer capacitors and batteries with high-energy/high-power carbon  
575 nanotube-based electrodes. *Journal of Materials Chemistry A*. **4** (38), 14586–14594 (2016).

576 40 Fang, B., Binder, L. A modified activated carbon aerogel for high-energy storage in electric  
577 double layer capacitors. *Journal of Power Sources*. **163** (1), 616–622 (2006).

578 41 Lei, C. et al. Activated carbon from phenolic resin with controlled mesoporosity for an  
579 electric double-layer capacitor (EDLC). *Journal of Materials Chemistry A*. **1** (19), 6037–6042  
580 (2013).

581 42 Lewandowski, A., Olejniczak, A., Galinski, M., Stepniak, I. Performance of carbon–carbon  
582 supercapacitors based on organic, aqueous and ionic liquid electrolytes. *Journal of Power*  
583 *Sources*. **195** (17), 5814–5819 (2010).

584 43 Dai, Z., Peng, C., Chae, J. H., Ng, K. C., Chen, G. Z. Cell voltage versus electrode potential  
585 range in aqueous supercapacitors. *Scientific Reports*. **5** (1), 9854 (2015).

586 44 Kang, B., Ceder, G. Battery materials for ultrafast charging and discharging. *Nature*. **458**  
587 (7235), 190–193 (2009).

588 45 Ban, C. et al. Nanostructured Fe<sub>3</sub>O<sub>4</sub>/SWNT Electrode: Binder-Free and High-Rate Li-Ion  
589 Anode. *Advanced Materials*. **22** (20), E145–E149 (2010).

590 46 Sun, Y., Hu, X., Luo, W., Xia, F., Huang, Y. Reconstruction of Conformal Nanoscale MnO on  
591 Graphene as a High-Capacity and Long-Life Anode Material for Lithium Ion Batteries. *Advanced*  
592 *Functional Materials*. **23** (19), 2436–2444 (2013).

593 47 Lou, X. W., Deng, D., Lee, J. Y., Feng, J., Archer, L. A. Self-Supported Formation of  
594 Needlelike Co<sub>3</sub>O<sub>4</sub> Nanotubes and Their Application as Lithium-Ion Battery Electrodes. *Advanced*  
595 *Materials*. **20** (2), 258–262 (2008).

596 48 Chen, L. et al. Electrochemical Stability Window of Polymeric Electrolytes. *Chemistry of*  
597 *Materials*. **31** (12), 4598–4604 (2019).

598 49 Ruschhaupt, P., Pohlmann, S., Varzi, A., Passerini, S. Determining Realistic Electrochemical  
599 Stability Windows of Electrolytes for Electrical Double-Layer Capacitors. *Batteries & Supercaps*. **3**  
600 (8), 698–707 (2020).

601 50 Kang, J. et al. Extraordinary Supercapacitor Performance of a Multicomponent and Mixed-  
602 Valence Oxyhydroxide. *Angewandte Chemie International Edition*. **54** (28), 8100–8104 (2015).

603 51 Pal, B., Yang, S., Ramesh, S., Thangadurai, V., Jose, R. Electrolyte selection for  
604 supercapacitive devices: a critical review. *Nanoscale Advances*. **1** (10), 3807–3835 (2019).

605 52 Xie, K. et al. Carbon Nanocages as Supercapacitor Electrode Materials. *Advanced*  
606 *Materials*. **24** (3), 347–352 (2012).

607 53 Demarconnay, L., Raymundo-Piñero, E., Béguin, F. A symmetric carbon/carbon  
608 supercapacitor operating at 1.6V by using a neutral aqueous solution. *Electrochemistry*  
609 *Communications*. **12** (10), 1275–1278 (2010).

610 54 Frackowiak, E. Carbon materials for supercapacitor application. *Physical Chemistry*  
611 *Chemical Physics*. **9** (15), 1774–1785 (2007).

612 55 Zhu, X. et al. Sustainable activated carbons from dead ginkgo leaves for supercapacitor  
613 electrode active materials. *Chemical Engineering Science*. **181**, 36–45 (2018).

614 56 Wang, Y. et al. Study on stability of self-breathing DFMC with EIS method and three-  
615 electrode system. *International Journal of Hydrogen Energy*. **38** (21), 9000–9007 (2013).

57 Xin, L., Zhang, Z., Qi, J., Chadderdon, D., Li, W. Electrocatalytic oxidation of ethylene glycol  
(EG) on supported Pt and Au catalysts in alkaline media: Reaction pathway investigation in three-  
electrode cell and fuel cell reactors. *Applied Catalysis B: Environmental*. **125**, 85–94 (2012).  
58 Fang, X., Kalathil, S., Divitini, G., Wang, Q., Reisner, E. A three-dimensional hybrid  
electrode with electroactive microbes for efficient electrogenesis and chemical synthesis.  
*Proceedings of the National Academy of Sciences*. **117** (9), 5074 (2020).  
59 Armstrong, E., sullivan, M., O'Connell, J., Holmes, J., O'Dwyer, C. 3D Vanadium Oxide  
Inverse Opal Growth by Electrodeposition. *Journal of The Electrochemical Society*. **162**, 605–612  
(2015).  
60 Wu, W.-Y., Zhong, X., Wang, W., Miao, Q., Zhu, J.-J. Flexible PDMS-based three-electrode  
sensor. *Electrochemistry Communications*. **12** (11), 1600–1604 (2010).  
61 Shitanda, I. et al. A screen-printed three-electrode-type sticker device with an accurate  
liquid junction-type reference electrode. *Chemical Communications*. **57** (23), 2875–2878 (2021).



Figure 1

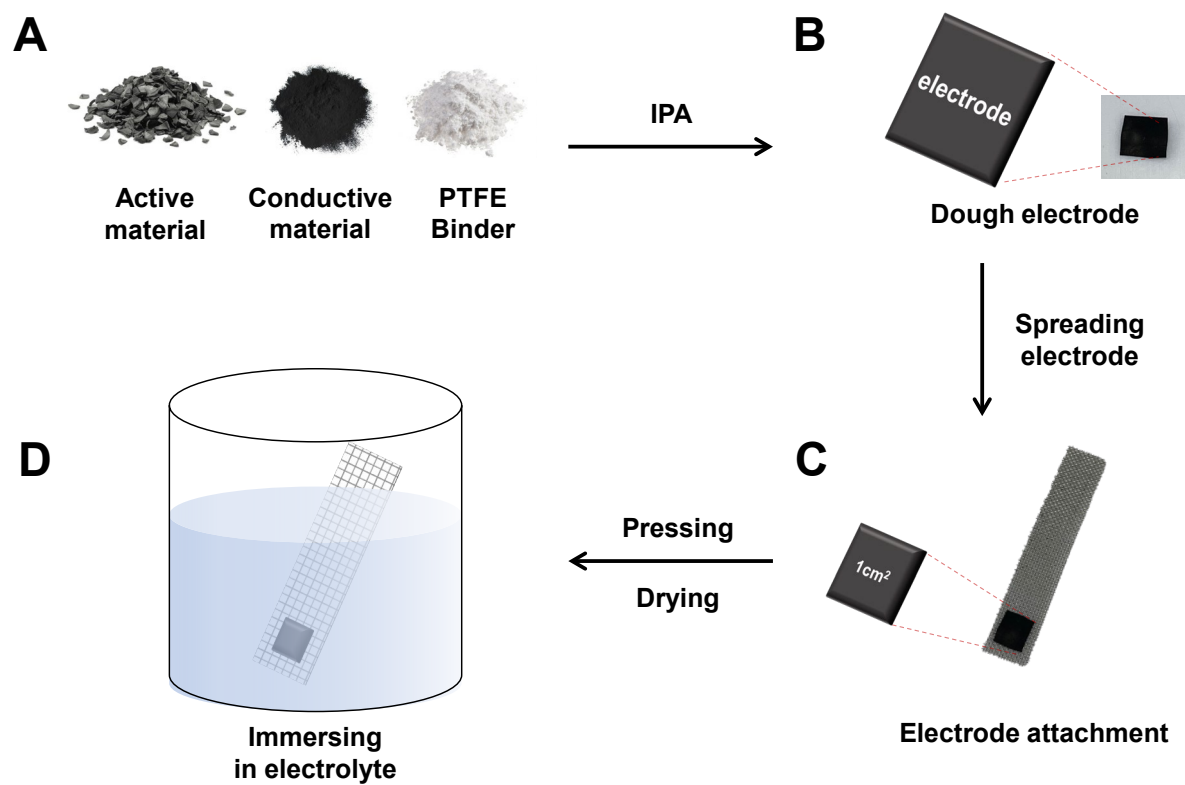


Figure 2

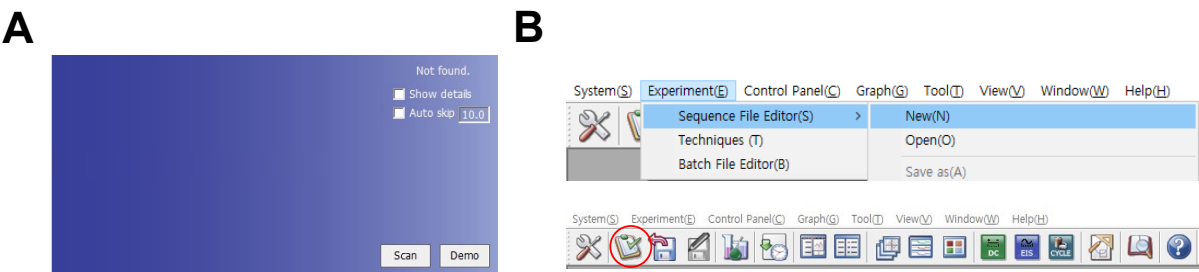
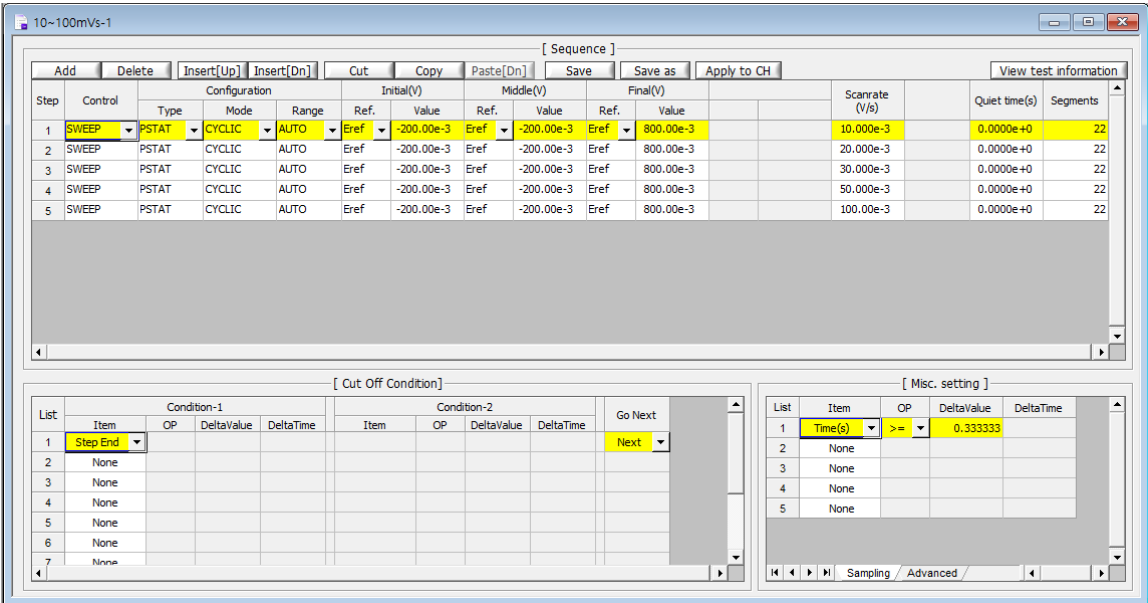


Figure 3

A



B

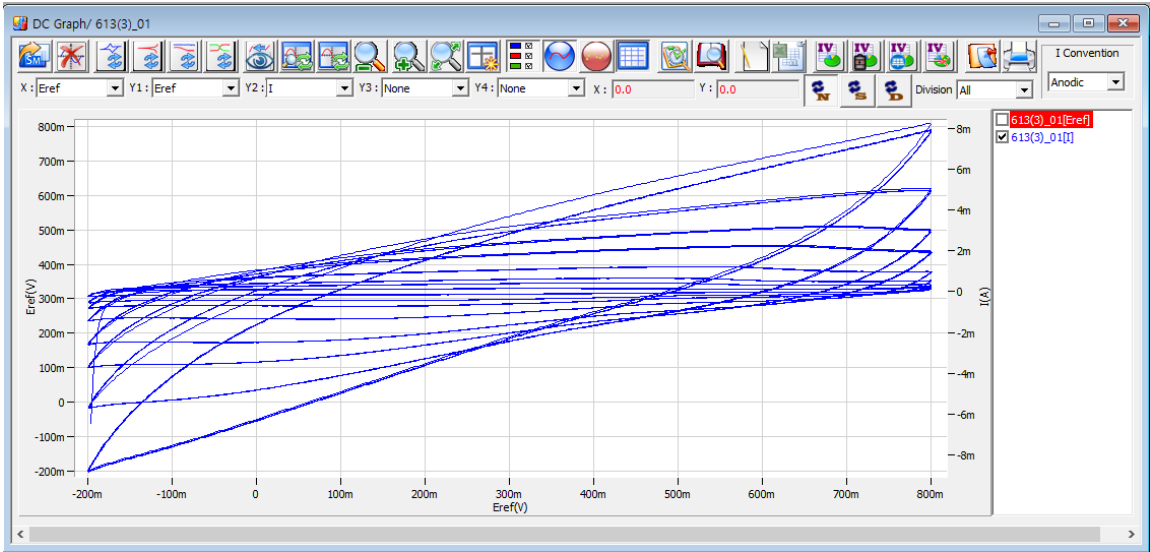
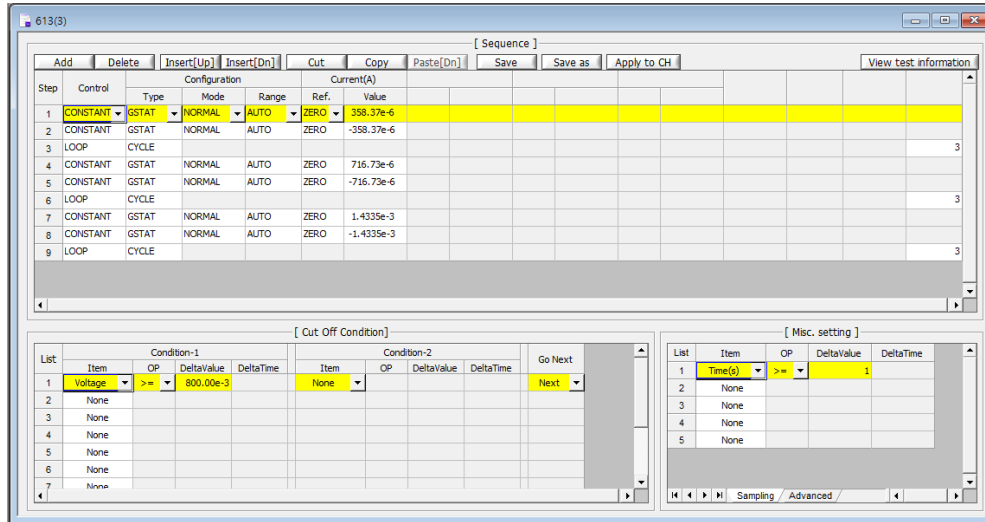
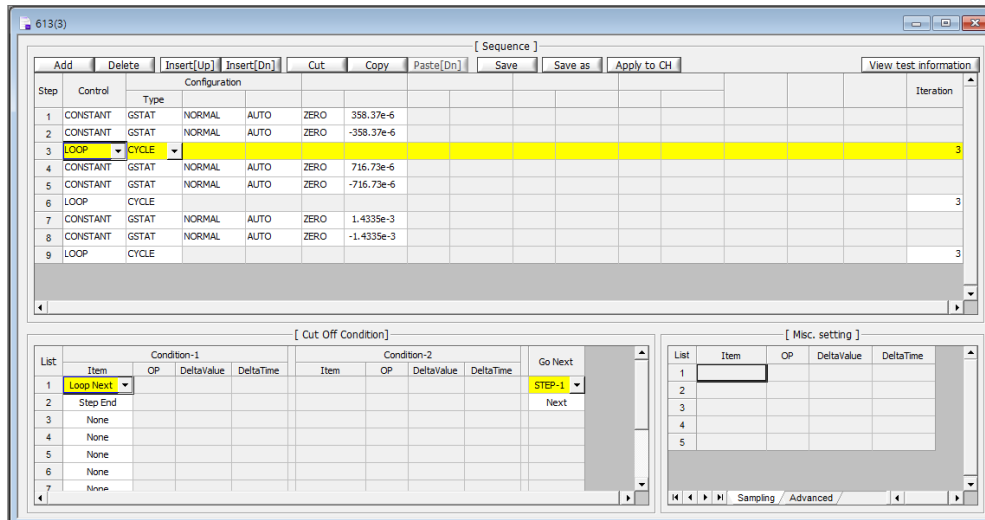


Figure 4

A



B



C

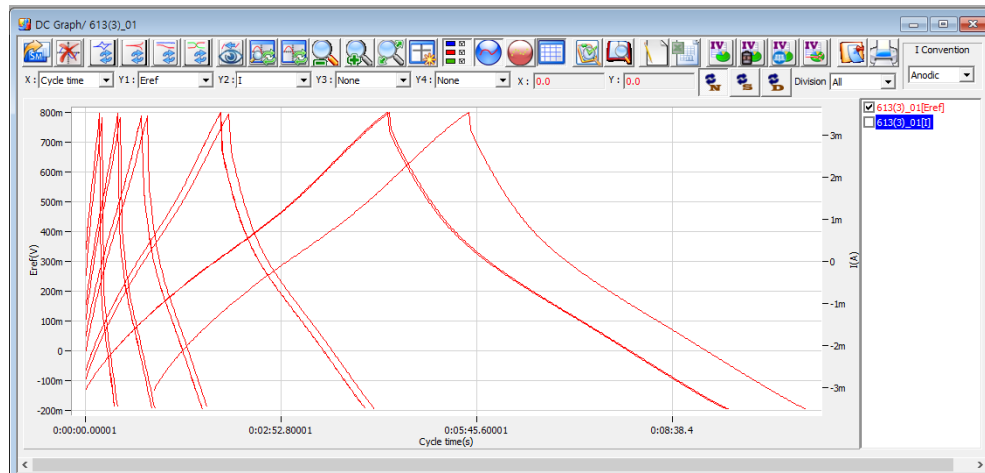
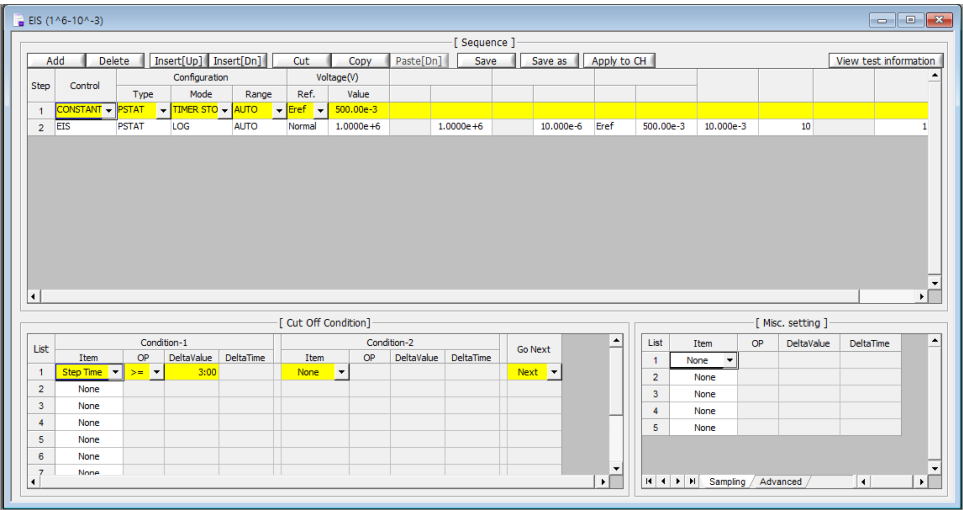
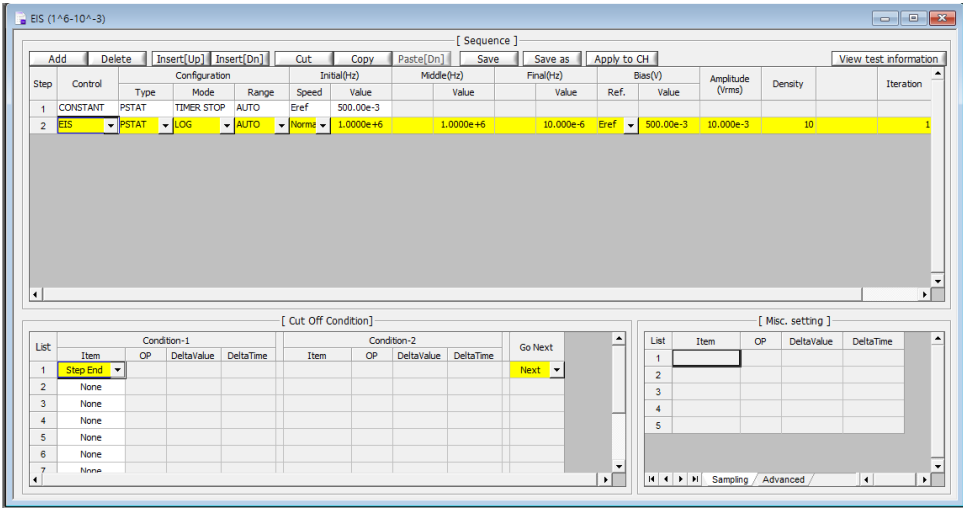


Figure 5

A



B



C

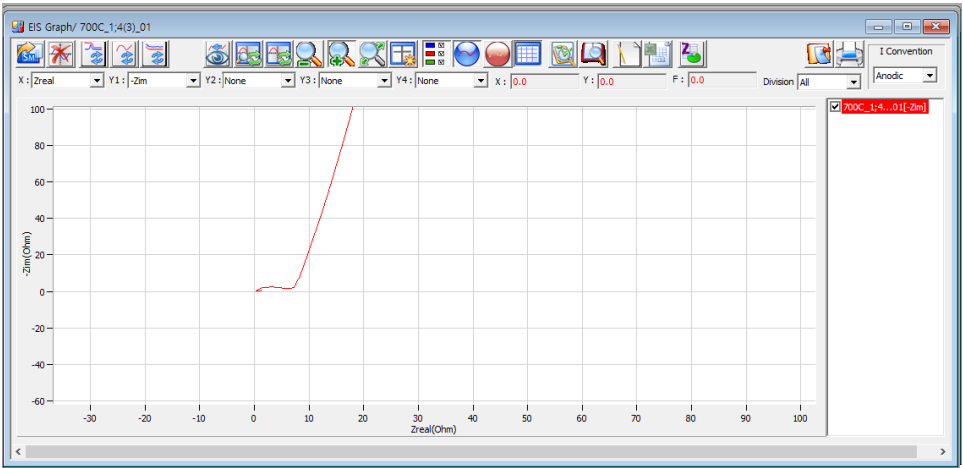


Figure 6

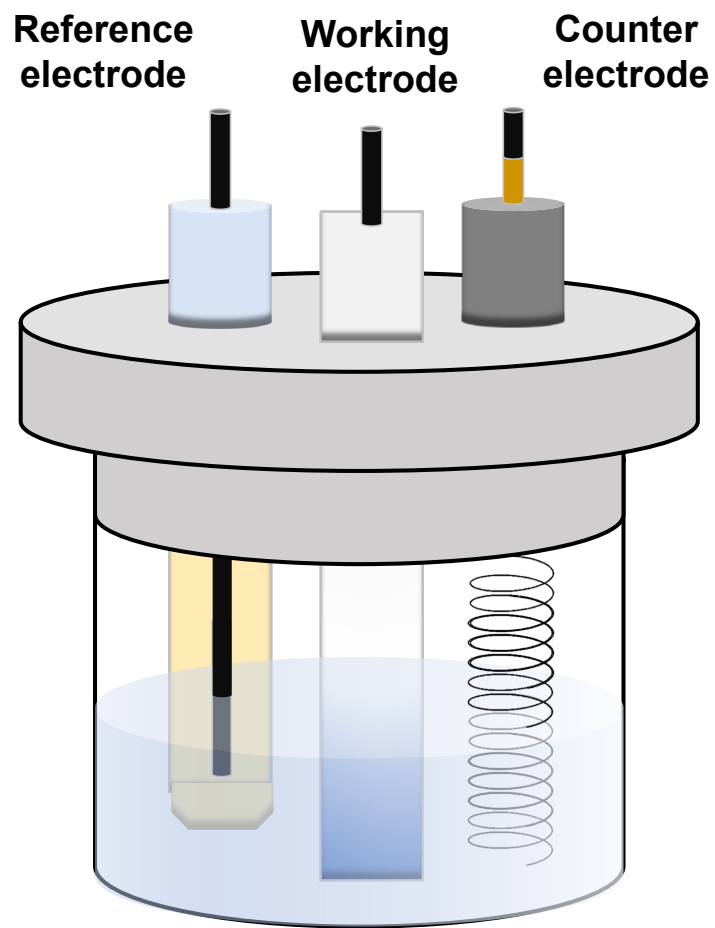
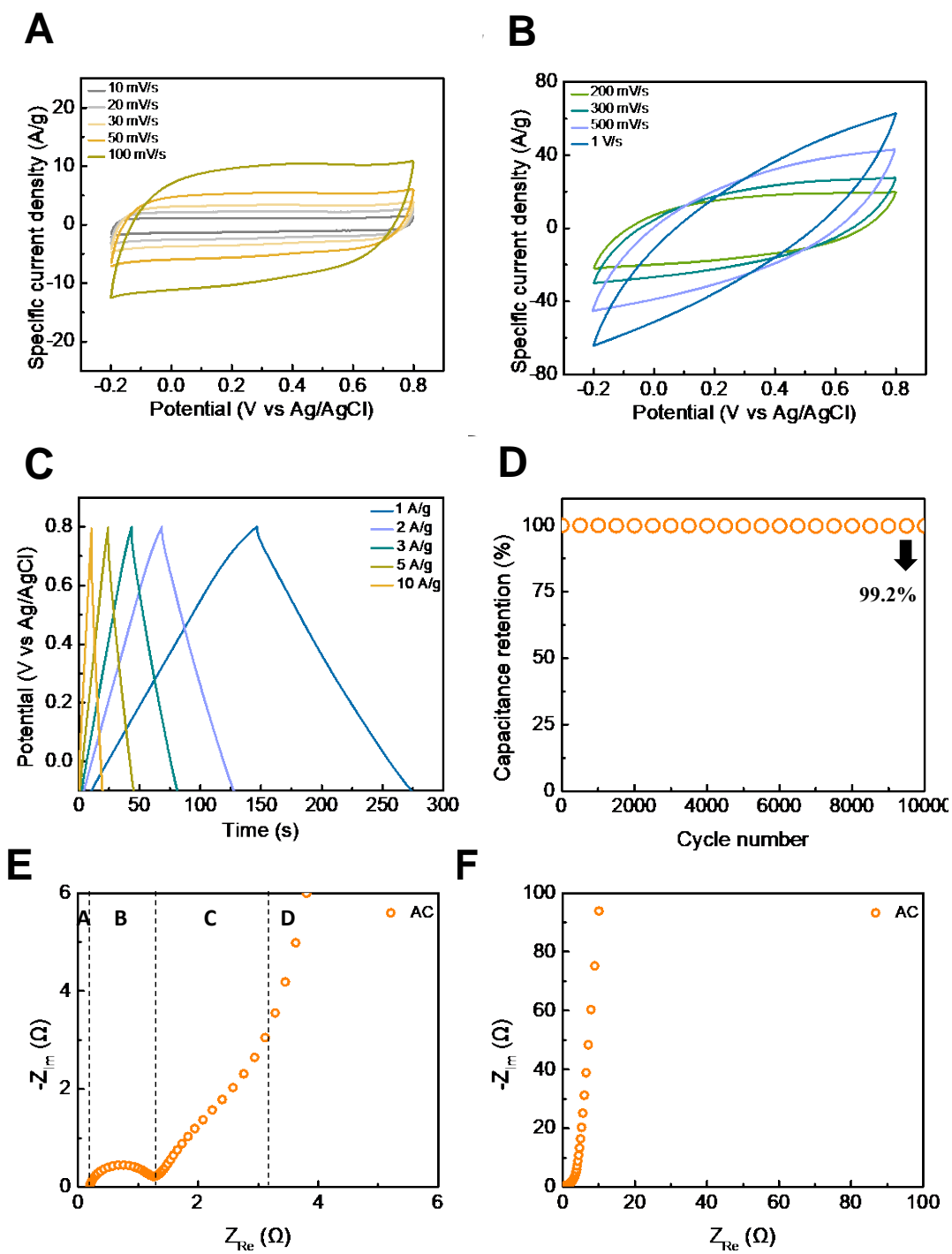


Figure 7







**Response to Referee's Comments**

Manuscript ID: JoVE63319

Title: Electrochemical analyses of supercapacitors using the three-electrode systems

We appreciate the constructive comments and suggestions from the referee, which were very helpful to improve the clarity of our manuscript. Based on the editor's comments, we have made changes to improve our manuscript. Consequently, we now believe that the quality of the manuscript is considerably improved to be suitable to publish in the *Journal of Visualized Experiments*. We have given a response to editor's comment, including the detailed changes that were highlighted in the manuscript.

**Response to the Editorial Comments:****Comment 1:**

The manuscript has been formatted as per the journal style, please retain.

Answer)

The manuscript was maintained in accordance with the format of the journal.

**Comment 2:**

Please approve/respond to specific comments made in the manuscript.

Answer)

The answers to the comment were added to the manuscript.

in *Page 2*

**Specific comment (1)** : Please also include in the Introduction the rationale behind the development and/or use of this technique.

Answer)

The reason why the three-electrode system is used and why it should be analyzed using it were added to the introduction.

in *Page 2 line 74*

The two-electrode system just gives information about the reaction between two electrodes. It is suitable for analyzing the electrochemical properties of the entire energy storage system. The potential of the electrode is not fixed. Therefore, it is not known at what voltage the reaction takes place. However, three-electrode system analysis only one electrode with fixing potential which can perform a detailed analysis of the single electrode. Therefore, the system is targeted toward analyzing the specific performance at the material level.

in *Page 4*

**Specific comment (2)** : Re-worded, please check.

Answer)

The revised contents did not undermine the original meaning.

in *Page 5*

**Specific comment (3)** : Are step-1~3, and Condition-1, a tab in the program?

Answer)

Yes. They are a tab in the program.

in *Page 5*

**Specific comment (4)** : What does below mean here?

Answer)

This means after step 4.

in *Page 5 line 213*

2.2.8. Step-1, -2, and -3 form a single loop. Copy and paste them after step-4 and change the value of Current (A) among  $3.7236\text{e-}3$ ,  $5.5855\text{e-}3$ ,  $9.3091\text{e-}3$ , and  $18.618\text{e-}3$ , which are calculated for various current densities of 2,3,5, and 10 A/g.

in *Page 6*

**Specific comment (5)** : Combined and re-worded, please check.

Answer)

The revised contents did not undermine the original meaning.

in *Page 7*

**Specific comment (6)** : Please remove the titles and Figure Legends from the uploaded figures. This information should be provided in the manuscript text. Include all the Figure Legends together at the end of the Representative Results in the manuscript text. Please define all abbreviations, symbols used in the figure in the figure legend.

Figure 2: Please blur out or remove all the commercial terms from the image.

Answer)

The Figure Legends was removed and added to the end of the manuscript representative results section. Also the commercial terms are blur in Figure 2.

in *Page 8*

**Specific comment (7)** : Corrected, please check.

Answer)

It has been corrected well.

in *Page 9*

**Specific comment (8)** : As we are a methods journal, please also include in the Discussion the following:

- a) Any limitations of the technique
- b) The significance with respect to existing methods
- c) Any future applications of the technique

Answer)

The limitation and future application of the three-electrode system and the significance of existing methods were added in the discussion section.

in *Page 10 line 455*

The three-electrode system can perform detailed analysis, but through this, all performance of the supercapacitor cannot be evaluated. As mentioned earlier, the three-electrode system analyzes only one electrode at the material level. The final supercapacitor system consists of symmetrical or asymmetric electrodes and requires further evaluation of this system for application to real-life and industry. Many studies have conducted an evaluation using a three-electrode and two-electrode system together. The system is also changing depending on the application. Not just evaluating supercapacitor, it is widely used in fuel cells and surface treatment fields. Various changes are taking place, such as giving flexibility or deviating from the existing form to another form. The materials' characteristics can be easily evaluated with this system. Therefore, it will be applied in various forms to fields that require material analysis and evaluation.

in *Page 9*

**Specific comment (9)** : To detect characteristics of what? The sentence seems incomplete, please check.

Answer)

The sentence has been modified.

in *Page 9 line 426*

If the current density is too high, the operating voltage is hardly measured. It is one of reason that the capacitance and energy density are decreased.

**Comment 3:**

Please remove all figures legends from the uploaded figure files and place them together in the manuscript text file after the representative results.

Answer)

More detailed information and specific action of each protocol were reflected in the manuscript.

*in Page 9 line 371*

**Figure 1.** Fabricating process of supercapacitor. (A) Prepare the materials for electrode and mix with IPA. (B) Make an electrode in the form of a dough. (C) Spread the electrode thinly, cut it into 1 cm<sup>2</sup> size with a thickness of 0.1–0.2 mm, and attach it to the stainless SUS. (D) Immerse the supercapacitor in electrolyte after pressing and drying.

**Figure 2.** Run the program for sequence settings. (A) Run the analysis program and (B) create the new sequence file with editor.

**Figure 3.** CV sequence settings. (A) CV sequence setting for each scan rate, and (B) real-time measurement CV graphs.

**Figure 4.** GCD sequence settings. (A, B) GCD sequence setting for each current density, and (C) real-time measurement GCD graphs.

**Figure 5.** EIS sequence settings. (A, B) EIS sequence setting, and (C) real-time measurement EIS graph.

**Figure 6.** Basic composition of the three-electrode system for electrochemical measurement.

**Figure 7.** Electrochemical analyses graphs; (A) CV at low scan rates (10 ~ 100 mV/s), (B) CV at high scan rates (200 ~ 1000 mV/s), (C) GCD at current density from 1 to 10 A/g, (D) long cycle test at current density of 10 A/g, and (E, F) EIS Nyquist plots.

**Comment 4:**

JoVE cannot publish manuscripts with commercial language, please blur out all commercial terms in figure 2.

Answer)

Commercial terms in Figure 2 were deleted.

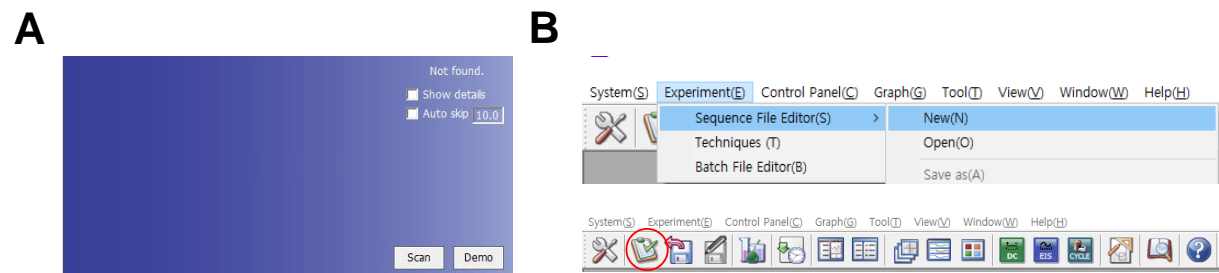


**Figure 2.** Run the program for sequence settings. (A) Run the analysis program and (B) create the new sequence file with editor.

**Comment 5:**

Once done, please thoroughly proofread the manuscript for any grammatical or spelling errors.

Answer)

The manuscript's grammar and typos were corrected once again.